COLLIMATION: EXPERIENCE AND PERFORMANCE

D. Mirarchi*, R.Bruce, M. Fiascaris, P. Hermes, A. Mereghetti, E. Quaranta, S. Redaelli,
A. Rossi, R. Rossi, B. Salvachua, G. Valentino, A. Valloni, J. Wagner,
CERN, Geneva, Switzerland
H. Garcia, R. Kwee-Hinzmann, Royal Holloway University of London, Egham, UK

Abstract

The main task of the LHC collimation system is to ensure safe and efficient operation, acting as first element of machine protection and minimizing the risk of magnet quenches induced by beam loss. The year 2016 has been very successful in terms of achieved LHC performance, thanks also to the reliability of its collimation system. No magnet quenches due to losses from circulating beam were recorded and an excellent cleaning inefficiency of about 10^{-4} with 6.5 TeV beams was achieved. The key elements in the set up of an efficient collimation system, together with the performance obtained with both proton and ion beams, are presented. Main operational improvements with respect to the 2015 run and plans for further upgrades are discussed. Highlights from collimation Machine Development (MD) studies and their implications on collimation performance on the different timescales are also reported.

INTRODUCTION

During the 2016 operation, a stored beam energy of more than 250 MJ was reached, as shown in Fig. 1. This large amount of stored energy was safely and efficiently handled by the collimation system [1] and no quenches from circulating beam loss were recorded. This achievement was made possible thanks also to the very good beam lifetime and orbit stability. On the other hand, the key contribution remained an efficient collimation system. The excellent precision and stability of the collimator alignment, which is performed during the initial commissioning after the winter shutdown (YETS), ensured more than in previous years operational efficiency. After the YETS a Beam Based Alignment (BBA) [2] is carried out for all the 86 movable collimators in the two LHC rings (i.e. without considering dump and injection protection collimators) both at injection and flat top [2]. Tertiary collimators (TCTP), acting as protection of the inner triplets in the four interaction points (IPs), are aligned also after the squeeze and with colliding beams. Detailed aperture measurements are performed during the initial commissioning and along the year, both at injection and with squeezed beams (both separated and colliding). Precise collimator settings, driven by functions, are then deployed based on the outcome of such measurements, and the system performance is fully validated through loss maps. Future operational scenarios and upgrades of the system are carefully studied during dedicated MDs, focusing on both the short-term and long-term operation of the collimation system. In this paper, the key aspects of these activities related to the commissioning of the LHC collimation system are reviewed.

* daniele.mirarchi@cern.ch

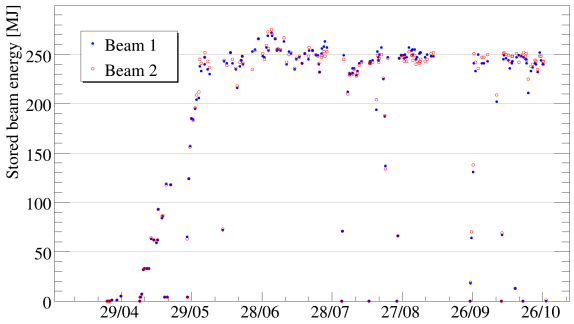

Figure 1: Stored energy in the LHC rings during the 2016 proton-proton physics run.

LHC APERTURE AND COLLIMATION SETTINGS

LHC aperture

A key parameter in the definiton of settings for the entire collimation system is represented by the available machine aperture. Detailed measurements are performed at injection and with squeezed beams (both separated and colliding). A new measurement technique was used in 2016 after a complete validation with respect to the previous technique used [3]. This new method allowed much faster and precise measurements. The main steps are:

1. A few pilot bunches are injected in the machine. Nominal bunches are also injected to establish the correct orbit, which are then blow out using the active transverse damper (ADT) [4].

2. All collimators are moved to parking position, and octupoles are switched off to minimize coupling between planes.

3. A selected bunch is gently excited in the desired plane (horizontal or vertical) using ADT until losses arise at the bottleneck.

4. A BBA of primary collimators (TCP) and/or TCTP is performed.

5. Overshoot of the BBA could lead to underestimation of the available aperture. Thus, the selected collimator is retracted of 0.1 σ and a gentle beam blowup is made.

Table 1: Measured available aperture at injection and with squeezed beams at $\beta^* = 40$ cm, together with the element where the bottleneck was found.

		Plane			
Date	**Config.**	**B1H [σ]**	**B1V [σ]**	**B2H [σ]**	**B2V [σ]**
3rd April	Inj.	12.5 - 13.0 (MBCR.4R8)	12.0 - 12.5 (Q6L4)	12.5 - 13.0 (TCDQM.4L6)	12.5 - 13.0 (Q4R6)
10rd April	Coll.	11.3 (Q3R5)	10.0 (Q3L1)	11.6 (Q3R1)	10.7 (Q3R1)
17rd April	Coll.	11.0 (Q3R5)	9.9 (Q3L1)	12.1 (Q3R1)	10.4 (Q3R1)

Table 2: Settings in 2016 of the entire collimation system at static points of the cycle.

Collimator		**Beam process**				
		Injection	**Flat top**	**End of Squeeze**	**Physics (XRP-OUT)**	**Physics (XRP-IN)**
Family	**IR**	[σ]	[σ]	[σ]	[σ]	[σ]
TCP	7	5.7	5.5	5.5	5.5	5.5
TCSG	7	6.7	7.5	7.5	7.5	7.5
TCLA	7	10	11	11	11	11
TCP	3	8.0	15.0	15.0	15.0	15.0
TCSG	3	9.3	18.0	18.0	18.0	18.0
TCLA	3	12	20.0	20.0	20.0	20.0
TCTP	1/2/5/8	13/13/13/13	23/37/23/23	9/37/9/15	9/37/9/15	9/37/9/15
TCL4/5/6	1/5	±25 [mm]	±25 [mm]	±25 [mm]	15/15/±25 [mm]	15/35/20
TCSP	6	7.5	8.3	8.3	8.3	8.3
TCDQ	6	8.0	8.3	8.3	8.3	8.3

This procedure is repeated until losses move again from the collimator to the bottleneck. For measurements at injection a reduced resolution of 0.5 σ is used.

6. Thus, the measured half-gap at the largest collimator opening where the losses were still at the selected collimator, represents the aperture of the bottleneck.

A selected subset of aperture measurement results at injection and with squeezed beams are reported in Table 1. The complete set of measurements can be found in [3,5,6]. Measurements at injection are consistent with the 2015 results, and the top-energy measurements with squeezed beams show a good agreement with the expectation from the scaling of the 2015 results at the same energy but with a $\beta^* = 80$ cm [7]. In both cases, the measured aperture were compatible with the nominal injection configuration and suitable for the proposed $\beta^* = 40$ cm for physics.

Collimation settings

Settings of the entire collimation system are defined depending on the available machine aperture in the various stages of the cycle. Taking into account the beam centres measured with the BBA, dedicated functions for all collimators are set up to connect different settings in each static points of the cycle [8]. This ensures an efficient collimation performance also during dynamic phases, such as the energy ramp, squeeze and adjust. The complete list of settings used during the 2016 operations is reported in Table 2. An overview of gaps for IR7 collimators in [mm] at injection and top energy is reported in Fig. 2. The main differences with respect to 2015 operation are:

- In 2016 the initial part of the squeeze is performed during the energy ramp, the so called *Ramp&Squeeze* [9]. Thus, TCTPs in IRs 1/5/8 are closed as protection of the inner triplet that represent the machine bottleneck already at flat top, with an aperture of about 27 σ. Complex changes of the crossing and separation bumps, that also depend on the β^*, also have to be accounted for. The corresponding setup is eased by the new Beam Position Monitors (BPM) functionality.

- The optimised phase advance between the beam dump kickers (MKD) and TCTPs allowed to reduce margins between the dump protection collimators (TCDQ) and TCTPs [10]. Thus, it was possible to close the TCTPs from 13.7 σ in 2015 with $\beta^* = 80$ cm, to 9.0 σ in 2016 with $\beta^* = 40$ cm.

- The collimation hierarchy in IR7 was also tightened, moving primary/secondary/tertiary collimators (TCP/TCSG/TCLA) from 5.5/8.0/14 σ in 2015 to 5.5/7.5/11 σ in 2016. The primary betatron cut was left unchanged to reduce the uncertainty on beam spike behavior during the cycle.

- Dump protection collimators TCDQ and TCSP were tightened consistently, from 9.1 σ to 8.3 σ in 2016. As in 2015, both TCDQ and TCSP are kept at the same settings.

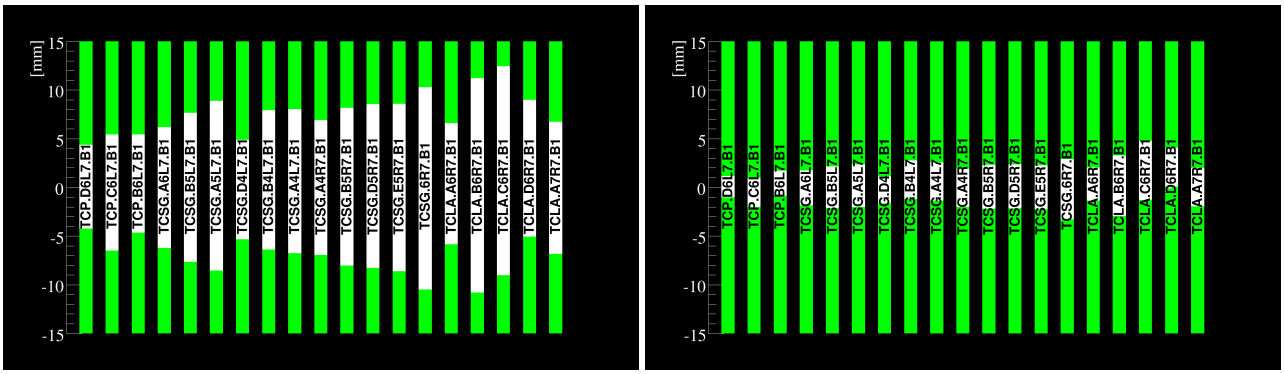

Figure 2: Overview of for IR7 collimators gaps in [mm] at injection (left) and top energy (right)

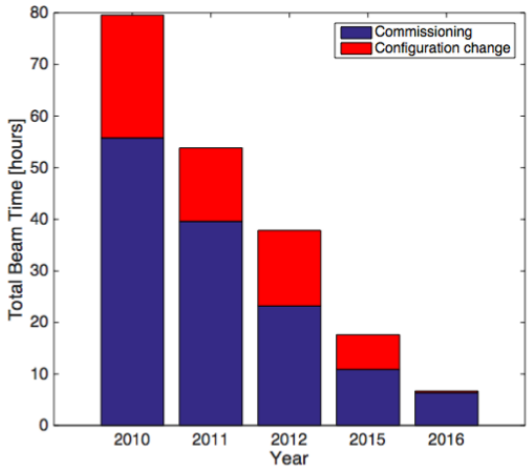

Figure 3: Time spent aligning collimators during the commissioning after the YETS (blue) and after changes of machine configuration (red).

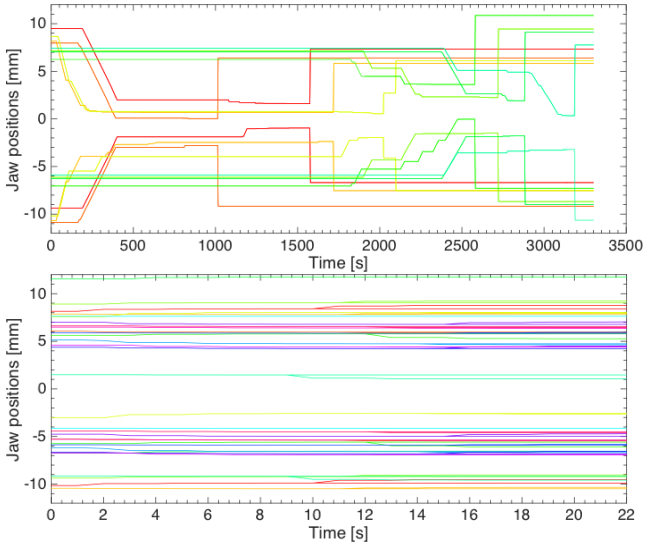

Figure 4: Alignment of TCTPs with BBA (top) and using parallelized alignment based on BPMs (bottom).

Luminosity debris collimators (TCL) are kept open until collisions are established. Only TCL4 and TCL5 and were moved to dedicated settings during the adjust beam process. The TCL5 were retracted when Roman Pots (XRP) of the forward physics experiment TOTEM [11] were put in place, to allow a larger mass spectrum reach. At the same time, TCL6 (placed after the XRPs) were then closed to provide an efficient absorption of physics debris.

COLLIMATION PERFORMANCE

Alignment

Significant improvements in the time needed for the collimator alignment were achieved. An overview of time spent for the alignment as a function of the year is shown in Fig. 3.

The blue bar in Fig. 3 includes the alignment of ring collimators in both beams, performed at injection and top energy after the YETS. More than 200 collimators were aligned in about 5 hours. The key upgrade was the higher acquisition rate of Beam Loss Monitor (BLM) signal, on which the feedback used for the BBA[1] is based.

[1] 100 Hz data were used in 2016, while 12.5 Hz data were used in 2015.

The red bar in Fig. 3 includes mainly alignment of TCTPs during changes of machine configuration along the year. Although the number of TCTPs alignments is about the same as in previous years, the amount of time spent in 2016 is almost invisible in Fig. 3. The main upgrade is the fully automated and parallelized alignment procedure based on BPM embedded in the four corners of the two collimator jaws of TCTPs and TCSPs [13, 14]. An example of the time needed to perform this alignment with and without BPMs is shown in Fig. 4. In previous years a BBA based on BLMs was needed. Thus, TCTPs (that are set at relatively large gaps) had to be carefully closed until the primary beam was touched. Using BPMs, the collimator jaws are moved just by the amount necessary to equalize the signals of the four BPMs. In conclusion, about 1 hour was needed to align the 8 TCTPs present in the ring using the BLM-based techniques, while less than 1 minute is required using BPMs and parallelizing the alignment of all the TCTPs. It is important to recall that in 2016 the commissioning time for machine configuration changes was therefore determined by the number of fills for validation.

Table 3: Qualification loss maps performed for the validation of the collimation system performance during the protons run, and number of fills required.

	Loss map		Fills	
Comm.	β	$\delta p/p$	**450 GeV**	**6.5 TeV**
YETS	100	12	2	4
TS1	20	3	2	1
TS2	24	5	2	2

Validation procedure

The cleaning performance of the system is evaluated through betatron and off-momentum loss maps. All of them (i.e. betatron in the two planes of both beams and both signs of $\delta p/p$) are performed at each static point of the cycle, during the initial commissioning after YETS.

Periodic validation of the system performance is carried out after each Technical Stop (TS), changes of machine configuration (such as change of crossing angle), or after the expiration of a validation period of 3 months (never attained in 2016). Only a subset of loss maps is requested for the most critical points of the cycle. Moreover, in 2016, betatron loss maps were performed for the first time during dynamic phases of the cycle (i.e. Ramp&Squeeze and Squeeze) after YETS, as part of required validation. This allowed to evaluate the system performance as a function of beam energy, and that the unprecedented $\beta^* = 40$ cm could be reached safely. An overview of the loss maps performed is reported in Table 3.

Betatron loss maps are carried out using the ADT, with which artificial and controlled high losses are generated. This is a very efficient procedure because it is possible to excite a single bunch in the plane of interest. Thus, it is possible to perform all loss maps in a single cycle.

A new method of off-momentum loss maps has been developed during 2015 and benchmarked with respect to the previous one during dedicated studies [12]. These loss maps are performed by applying an RF frequency shift that brings the beam on a off-momentum orbit. A frequency shift smaller than in previous years is now applied. However, a faster trim is used and feedbacks on BLMs signal were put in place to stop this RF shift and restore the nominal RF frequency. Thus, it is now possible to perform both signs of off-momentum loss maps in the same fill (possibly leaving enough beam for an asynchronous dump test), whereas a dedicated fill for each off-momentum loss map was needed previously. This led to a significant reduction of time and number of fills required. Indeed, despite the largest number of loss maps performed in 2016 with respect to previous years, the smallest number of fill was necessary. The number of fills needed could be further reduced by simplifying the machine cycle, reducing fixed points were a significant amount of time could be spent during operations.

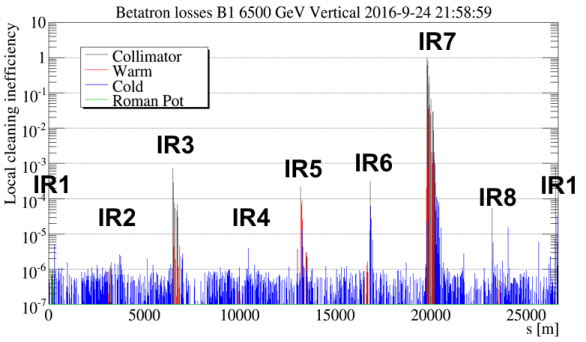

Figure 5: Example of betatron loss map performed in physics for the vertical plane of beam 1. The losses on collimators are shown by black bars, while cold and warm elements are displayed in blue and red, respectively. Losses on Roman Pot are reported in green.

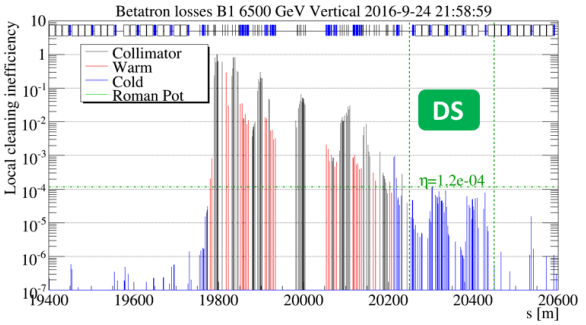

Figure 6: Zoom on IR7 of the betatron loss maps shown in Fig. 5. The magnetic lattice is shown on top, where collimators are reported as black bars, while quadruple and dipole magnets are shown as blue and white boxes.

Cleaning

An example of betatron loss map performed in physics for the vertical plane of beam 1 is shown in Fig. 5. Only BLM ionization chamber are used, and the background is subtracted. The local cleaning inefficiency in each point of the machine is then evaluated as:

$$\eta_i = \frac{BLM_i}{BLM_{TCP}} \,. \tag{1}$$

As clearly visible in Fig. 5 the limiting location of the entire ring in terms of losses is represented by the Dispersion Suppressor (DS) of the betatron cleaning insertion (IR7). A zoom of the IR7 is reported in Fig. 6, and the cleaning performance of the system is given by the highest normalized losses in the DS.

A summary of the cleaning inefficiency with 6.5 TeV proton beams during the Run II is reported in Fig. 7. A good stability of performance along the years is observed. In 2016 a tighter collimation hierarchy than in 2015 was present. The improvement of cleaning with these new settings is clearly visible. Note that such performance is obtained with only one alignment per year. Only betatron cleaning performance of the system are discussed here and a complete overview

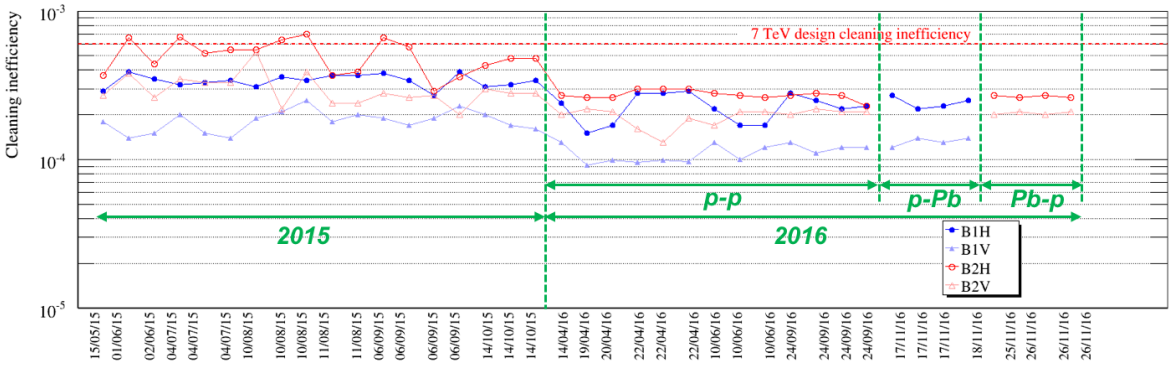

Figure 7: Summary of the betatron cleaning performance with 6.5 TeV proton beams during the Run II, in both planes of both beams. Cleaning measured during the proton-lead ion runs in 2016 are also reported.

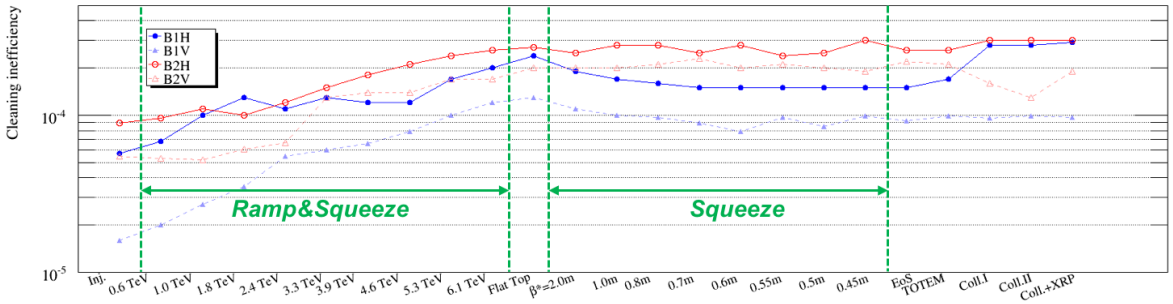

Figure 8: Summary of the betatron cleaning during the entire cycle for protons.

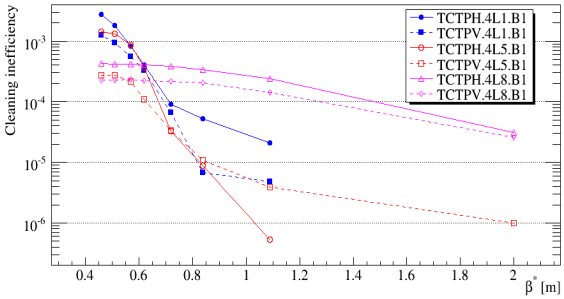

Figure 9: Normalized losses on TCTPs during the squeeze.

of all qualification loss maps, including off-momentum, can be found in [15].

A summary of the cleaning performance along the entire cycle is shown in Fig. 8. The expected worsening of efficiency as a function of energy is observed, while the performance is stable after flat top. Note that the IR7 optics remains constant after flat top, and cleaning is expected to be also constant. The change of inefficiency observed in the horizontal plane of beam 1 during the squeeze was given by a small bump (of about 100 μm) building up toward the TCLAs, which was corrected by the orbit feedback only while establishing collisions in IP1 and IP5. This was corrected during TS1, and a B1H loss map was performed at $\beta^* = 55$ cm as test. The cleaning measured was then consistent with respect to values at flat top and in collisions (i.e. 2.0×10^{-4}). Betatron loss maps during dynamic phases

Table 4: Qualification loss maps performed for the validation of the collimation system performance during the ions run, and number of fills required.

Comm.	Loss map β	Loss map $\delta p/p$	Fills Inj.	Fills Top En.
4 Z TeV (p-Pb)	20	6	2	2
6.5 Z TeV (p-Pb)	16	4	0	2
6.5 Z TeV (Pb-p)	24	8	2	2

of the cycle can allow to identify even very small drifts from the ideal machine configuration, while the collimators are moved according to predefined functions.

Another useful outcome of continuous loss maps during the squeeze was the possibility to monitor losses on TCTPs while going to $\beta^* = 40$ cm. Normalized losses on TCTPs for horizontal loss maps of beam 1 are reported in Fig. 9. This represents both a useful input for the benchmarking of beam loss pattern simulations, and a confirmation that losses on TCTPs were under control during the squeeze.

ION BEAMS COLLIMATION

Different activities were carried out during the various phases of the lead ions run. The proton-lead ions run in 2016 was particularly demanding because it involved two beam energies (4 Z TeV and 6.5 Z TeV) and different particle species circulating in the two rings. Protons and lead ions were injected in beam 1 and beam 2, respectively, for the 4

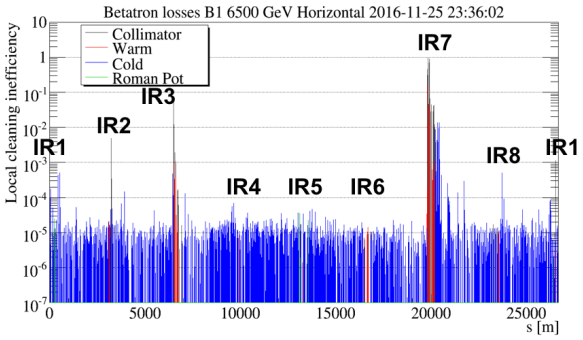

Figure 10: Example of betatron loss map performed in physics for the horizontal plane of beam 1 with Pb ion beams.

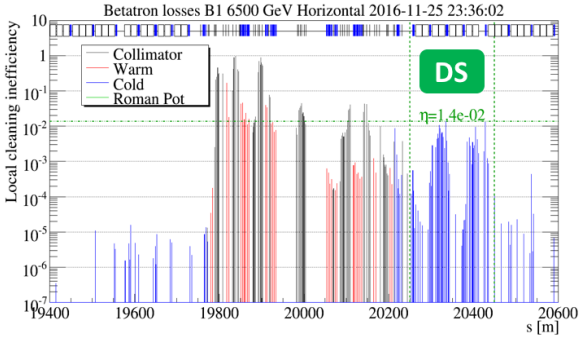

Figure 11: Zoom on IR7 of the betatron loss maps shown in Fig. 10.

Z TeV physics. Same injection configuration was used in the first part of the 6.5 Z TeV physics. Finally, beam species were switched once the required integrated luminosity was reached. All these changes of machine configuration took place in about one month.

In order to provide an efficient collimation performance and ensure the machine safety during the 4 Z TeV physics, all collimator ramp functions had to be redone, and alignment and function generation had to be done also for the TCTPs at flat top and in collision.

Regarding the 6.5 Z TeV physics, the same ramp functions as deployed for the 6.5 TeV proton-proton physics could be used. The main activities carried out were the alignment and function generation of TCTPs at: Flat Top (new β^* after combined Ramp&Squeeze), End of Squeeze and Collisions.

An overview on the qualification loss maps performed in the different commissioning phases is reported in Table 4. The minimum set of required loss maps was performed, given the relatively short time of the ion run. For example, qualification loss maps at injection for the 6.5 Z TeV physics with the same beam configuration as for the 4 Z TeV were not performed.

As for the proton-proton physics configuration, the cleaning performance of the system is evaluated through betatron and off-momentum loss maps. An example of a betatron loss map performed in physics at 6.5 Z TeV for the horizontal plane of beam 1 is shown in Fig. 10. The IR7-DS is still the

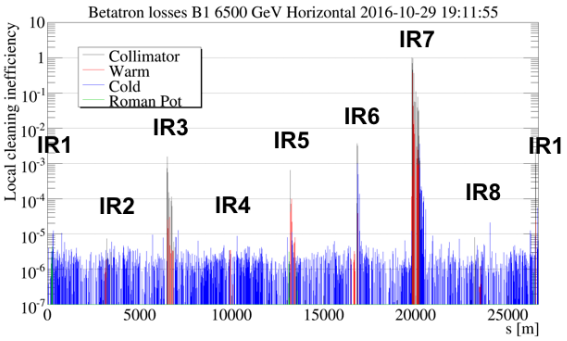

Figure 12: Example of betatron loss map with ATS optics, $\beta^* = 33$ cm and colliding beams for the horizontal plane of beam 1.

limiting location in terms of losses around the entire ring. However, other significant loss peaks around the ring are present, which are due to ion fragments with different rigidity that are able to emerge from the IR7 insertion [16, 17]. A significantly worse cleaning than with protons (about a factor 100 worse) is observed, which is mainly due to fragmentation and dissociation processes that take place in the collimator jaws. A zoom of the IR7 insertion is reported in Fig. 11.

A summary of the cleaning performance with lead ion beams during Run II is reported in Fig. 13. The cleaning performance of the system remains relatively constant along the years, regardless of changes of collimator settings and beam energy.

HIGHLIGHTS FROM COLLIMATION MDs

A large variety of Machine Development (MD) studies were performed and supported by the collimation team in 2016, with topics related to both the short-term and long-term operation of the collimation system. Regarding outcomes already used to improve the operational efficiency in 2016, the collaboration with BE-OP and BE-BI led to the development of a new FESA class for the control of losses during off-momentum loss maps. Key topics of 2016 MDs useful for the proposal of collimators settings for 2017 operation [6] were:

- Collimation hierarchy limits [18].
- Single collimators impedance [19].
- Operation with TCPs at tighter settings [20].
- Detailed IR aperture measurements [3].
- TCTPs induced background [21].

Studies of collimation aspects of ATS optics, such as cleaning performance and aperture measurement, were also performed within the ATS optics MDs [22]. An example of a loss map with ATS optics, $\beta^* = 33$ cm and colliding beams,

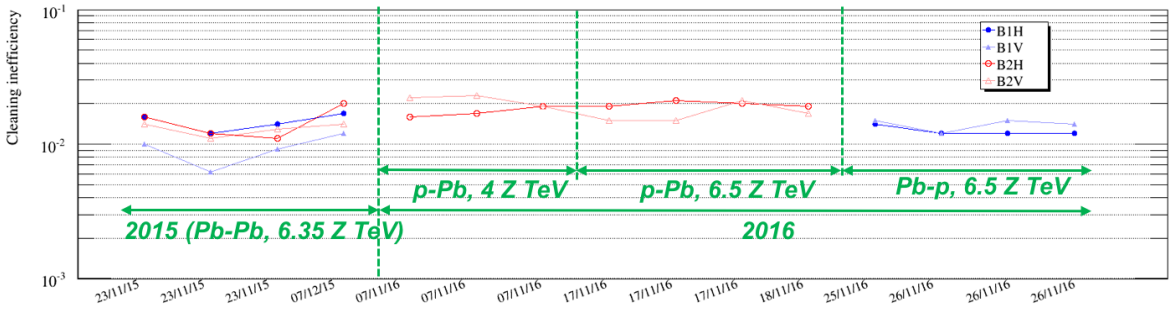

Figure 13: Summary of the betatron cleaning performance with ion beams during the Run II, in both planes of both beams.

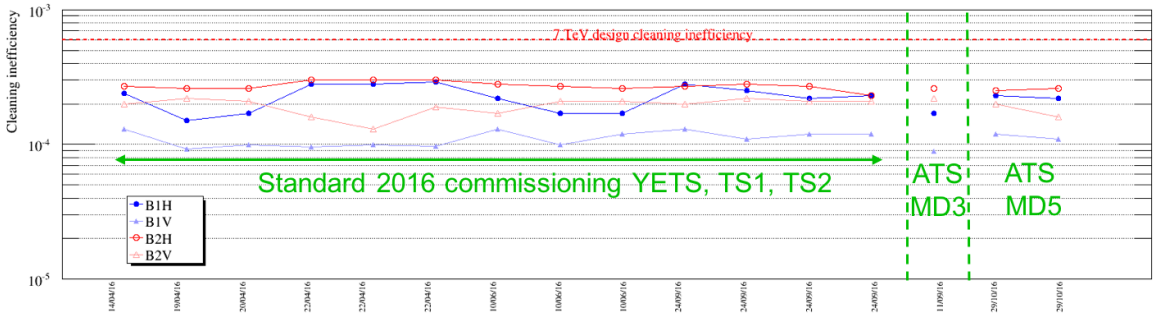

Figure 14: Summary of the betatron cleaning performance with 6.5 TeV beams during the Run II, in both planes of both beams. Cleaning measured during the proton-lead ion runs in 2016 are also reported.

is shown in Fig. 12. The beam loss patterns observed for both planes and both beams do not shown any concern in terms of spurious losses around the ring. A comparison with respect to cleaning efficiency obtained with the present optics and ATS is reported in Fig. 14. Consistent collimation performance is observed with both optics.

Regarding studies for possible applications in the High Luminosity upgrade of the LHC (HL-LHC) [23], the main topics treated were:

- Crystal collimation, where cleaning performance and channeling stability during dynamic phases of the machine were measured [24].
- Halo scraping, useful for measurement of diffusion speed and tail population in view of scaling to HL-LHC beam intensity [25].
- Active halo control, considering both narrow band excitation and tune ripple methods [26, 27].
- Coronagraph, that aims to a non-destructive halo population measurements [28].

CONCLUSIONS

A safe and efficient LHC operation was ensured by the collimation system in 2016. No magnet quenches due to beam loss were recorded, with more than 250 MJ of stored energy routinely in the machine. The main elements in the set up of an efficient collimation system, together with the performance obtained with both protons and ions beam, were presented. A stable cleaning inefficiency of about 10^{-4} with 6.5 TeV beams was achieved along the entire year, with a single collimator alignment. The cleaning inefficiency is increased to about 10^{-2} with ion beams.

Key improvements such as faster BLMs acquisition rate, automatic and parallelized TCTPs alignment based on BPMs, and a new off-momentum loss map procedure, lead to a significant reduction of time needed for collimation activities during the various commissioning phases.

Highlights from collimation MDs were also reported.

ACKNOWLEDGMENT

The authors would like to thank the BE-OP group for the support during measurements, the BE-ABP group for the useful internal discussions and the BE-BI group for being “our eyes”.

REFERENCES

[1] R. Assmann et al.,"The final collimation system for the LHC", Proceedings of EPAC 10, Edinburgh, UK USA; LHC-PROJECT-Report-919; CERN-LHC-Project-Report-919

[2] G. Valentino et al.,"Semiautomatic beam-based LHC collimator alignment.", PRST-AB 15.5 (2012): 051002.

[3] R. Bruce et al.,"Detailed IR aperture measurements", CERN-ACC-NOTE-2016-0075

[4] W. Hofle et al., "Controlled Transverse Blow-UP of high-energy proton beams for aperture measurements and loss maps", Proceedings of IPAC12, N. Orleans, USA, pp. TH-PPR039

[5] P. Hermas et al.,"Summary of aperture measurements", LHC Collimation Working Group #204

[6] R. Bruce et al.,"Beta* reach for the different scenarios", 7th Evian Workshop

[7] R. Bruce et al.,"LHC Machine Configuration in the 2016 Proton Run", LHC Performance Workshop, Chamonix 2016

[8] R. Bruce, R. W. Assmann, and S. Redaelli, "Principles for generation of time-dependent collimator settings during the LHC cycle", in Proceedings of IPAC11, San Sebastian, Spain, pp. THPZ029

[9] M. Solfaroli Camillucci et al.,"Combined Ramp and Squeeze to 6.5 TeV in the LHC", Proceeding of IPAC16, Busan, Korea, pp.TUPMW031

[10] R. Bruce et al.,"Reaching record-low β^* at the CERN Large Hadron Collider using a novel scheme of collimator settings and optics", NIM A, 2016

[11] G. Anelli et al.,"The totem experiment at the CERN Large Hadron Collider", JINST, 3.08 (2008) S08007.

[12] B. Salvachua et al., "Validation of Off-momentum Cleaning Performance of the LHC Collimation System", Proceeding of IPAC16, Busan, Korea, WEPMW007

[13] G. Valentino et al.,"Successive approximation algorithm for beam-position-monitor-based LHC collimator alignment" PRST-AB, 17.2 (2014): 021005.

[14] A. Dallocchio et al.,"LHC collimators with embedded beam position monitors: a new advanced mechanical design", Proceeding IPAC11, San Sebastian, Spain, pp.TUPS035

[15] D. Mirarchi et al.,"Status of loss maps and validation", LHC Collimation Working Group #204

[16] P. Hermes et al.,"2016 studies of beam cleaning with lead ions", LHC Collimation Working Group #211

[17] P. Hermes et al.,"Measured and simulated heavy-ion beam loss patterns at the CERN Large Hadron Collider", NIM A 819 (2016) 73?83

[18] A. Mereghetti et al.,"MD1447: Beta*-reach: IR7 Collimation Hierarchy Limit and Impedance", to be published in 2017

[19] A. Mereghetti et al.,"MD1875: Impedance Contribution of Single Collimators", to be published in 2017

[20] D. Mirarchi et al.,"MD1878: Operation with primary collimators at tighter settings", to be published in 2017

[21] R. Bruce et al.,"Tertiary collimator closure test in physics", CERN-ACC-NOTE-2016-0076

[22] S. Fartoukh et al.,"ATS MD's in 2016", CERN-ACC-2017-0003

[23] B. Alonso and L. Rossi,"HiLumi LHC Technical Design Report", CERN-ACC-2015-0140

[24] R. Rossi et al.,"MD1879: Crystal Channeling in Dynamic Operational Phases", to be published in 2017

[25] G. Valentino et al.,"MD1291: Beam halo population measurements using collimator scans", to be published in 2017

[26] J. Wagner et al.,"MD1388: Active Halo Control through narrow-band excitation with the ADT at injection", to be published in 2017

[27] H. Garcia et al.,"MD 1691: Active halo control using tune ripple at injection", to be published in 2017

[28] G. Trad et al.,"MD1900: Measuring the beam halo population via SR Coronagraph", to be published in 2017